Title

Facile Strategy Enabling Both High Loading and High Release Amounts of the Water-Insoluble Drug Clofazimine Using Mesoporous Silica Nanoparticles

Journal

ACS Applied Materials & Interfaces, 10(38)

ISSN

1944-8244

Authors

Chen, Wei
Cheng, Chi-An
Lee, Bai-Yu
et al.

Publication Date

2018-09-26

DOI

10.1021/acsami.8b09069

A Facile Strategy Enabling Both High Loading and High Release Amounts of the Water-insoluble Drug Clofazimine Using Mesoporous Silica Nanoparticles

Journal:	*ACS Applied Materials & Interfaces*
Manuscript ID	am-2018-09069h.R2
Manuscript Type:	Article
Date Submitted by the Author:	25-Aug-2018
Complete List of Authors:	Chen, Wei; University of California Los Angeles, Chemistry Cheng, Chi-An; University of California Los Angeles , Bioengineering Lee, Bai-Yu; University of California, Los Angeles, Medicine Clemens, Daniel; University of California, Los Angeles, Department of Medicine Huang, Wen-Yen; University of California Los Angeles, Chemistry and Biochemistry Horwitz, Marcus; UCLA, Medicine Zink, Jeffrey; UCLA, Chemistry and Biochemistry

A Facile Strategy Enabling Both High Loading and High Release Amounts of the Water-insoluble Drug Clofazimine Using Mesoporous Silica Nanoparticles

Wei Chen,[†,§,‡] *Chi-An Cheng,*[$,§,‡] *Bai-Yu Lee,*[#] *Daniel L. Clemens,*[#] *Wen-Yen Huang,*[†,§] *Marcus A. Horwitz,*[#] *Jeffrey I. Zink*[†,§,*]

† Department of Chemistry & Biochemistry, University of California, Los Angeles, California 90095, United States

$ Department of Bioengineering, University of California, Los Angeles, California 90095, United States

§ California NanoSystems Institute, University of California, Los Angeles, California 90095, United States

Division of Infectious Diseases, Department of Medicine, University of California, Los Angeles, California 90095, United States

‡ These authors contributed equally

KEYWORDS

Mesoporous silica nanoparticles, drug delivery, water-insoluble drugs, clofazimine, tuberculosis, chaperone

ABSTRACT

The use of nanocarriers to deliver poorly soluble drugs to the sites of diseases is an attractive and general method, and mesoporous silica nanoparticles (MSNs) are increasingly being used as carriers. However, both loading a large amount of drugs into the pores and still being able to release the drug is a challenge. In this paper we demonstrate a general strategy based on a companion molecule that chaperones the drug into the pores and also aids it in escaping. A common related strategy is to use a miscible co-solvent DMSO, but although loading may be efficient in DMSO, this co-solvent frequently diffuses into an aqueous environment leaving the drug behind. We demonstrate the method by using acetophenone (AP), an FDA approved food additive as the chaperone for clofazimine (CFZ), a water-insoluble antibiotic used to treat leprosy and multidrug-resistant tuberculosis. AP enables high amount of CFZ cargo into the MSNs and also carries CFZ cargo out from the MSNs effectively when they are in an aqueous bio-relevant environment. The amount of loading and the CFZ release efficiency from MSNs were optimized; 4.5 times more CFZ was loaded in MSNs with AP than that with DMSO and 2300 times more CFZ was released than that without the assistance of the AP. *In vitro* treatment of macrophages infected by *Mycobacterium tuberculosis* with the optimized CFZ-loaded MSNs killed the bacteria in the cells in a dose-dependent manner. These studies demonstrate a highly efficient method for loading nanoparticles with water-insoluble drug molecules and the efficacy of the nanoparticles in delivering drug into eukaryotic cells in aqueous media.

1. Introduction

Poor water solubility of drug molecules is a significant problem because almost 40% of the newly discovered drug molecules are hydrophobic which reduces their bioavailability and thus suppresses their efficacy.[1] Great effort has been devoted to solving the problem of getting them to the site of the disease. One important strategy is to use nanomaterials as carriers to deliver

insoluble drugs.[2] Mesoporous silica nanoparticles (MSNs) have aroused much attention in this regard because their properties include high surface area (about 1000 m^2/g), large pore volume (1 cc/g), tunable pore sizes (2-20 nm), easy surface functionalization, and high biocompatibility.[3–12] These excellent intrinsic properties enable MSNs to carry a wide variety of cargos, including drugs,[13–17] genes,[18–21] proteins,[22,23] and other biomolecules for *in vitro* or *in vivo* biomedical applications.[24,25] Additionally, MSNs can incorporate fluorescence and magnetic properties, and simultaneously serve as image contrast agents by integrating the relevant functional materials for diagnostics and therapeutics.[26–28] Accordingly, these preeminent "theranostic" (therapeutic plus diagnostic) nanoparticles, serving as the excellent nanocarriers, are being broadly explored in biomedical applications.[29–35]

The major challenges are to get the insoluble drug into the pores and then allow the drugs to escape. One of the most widely-used methods to load the poorly water-soluble drugs in MSNs is to dissolve the drugs in dimethyl sulfoxide (DMSO).[14] The loading step is done by soaking MSNs in the DMSO solution which allows the drug molecules to diffuse into the channels of MSNs efficiently. After the loading step, the drug-loaded MSNs are washed with water or buffer solutions thoroughly to remove DMSO from the pores. However, during this washing step, some of drugs may be removed as well considering weak interactions between the hydrophobic drug molecules and the hydrophilic porous surface, thus decreasing the loading weight percent of drugs (defined as (weight of drugs / weight of MSNs) x 100%).[2,14] To attempt to solve this problem of low drug loading, the channels of MSNs were functionalized with hydrophobic groups to increase the hydrophobic interactions between the drugs and the channels.[36,37] However, those further surface modifications complicate the delivery systems and lead to colloidal instability in aqueous environment. Another critical challenge that remains is that the

amount of the hydrophobic drug released from the carriers into an aqueous environment is poor, even though MSNs are able to carry the drugs to the location of a disease.[36–38] Consequently, the bioavailability of the drugs may be reduced to a level insufficient for effective treatment, or an extremely high dosage of the particles may be required to achieve a sufficient local concentration of free drug for it to be effective. Hence, to enhance the bioavailability of the drug, it is essential to improve its release efficiency from the nanocarriers.

Hydrotropy is a technique that increases the water solubility of water insoluble molecules by adding a second solute (*i.e.* hydrotrope).[39,40] Hydrotropes are short chain amphiphilic molecules, usually containing both the hydrophobic and hydrophilic moieties in their chemical structures, in which the hydrophobic part interacts with water-insoluble drugs through hydrophobic interactions, and the hydrophilic part helps solubilize the drug-hydrotropes complexation structure in water. The hydrotrope-assisted solubilization of water-insoluble drugs in water possesses a signature feature of a sigmoidal solubility curve.[41,42] At low concentration of hydrotropes, the solubility of water-insoluble drugs hardly increases. The solubility of water-insoluble drugs significantly increases above a certain hydrotrope concentration, usually called a minimum hydrotrope concentration (MHC), when self-aggregation of the hydrotropes happens.[42,43] Other mechanisms may also involve in the hydrotrope-assisted solubilization of water-insoluble drugs.[44–47] Two advantages of using hydrotropy are that it obviates the need for chemical modification of the drugs, which may interfere with pharmaceutical activity; and it does not require a specific formulation for emulsification. The water solubility of water-insoluble drugs could be enhanced from several folds to several orders of magnitude by the hydrotrope-assisted solubilization especially if the hydrotropes associate well with the drugs.[40,41,48]

In this study, we choose clofazimine (CFZ) as an example of a water-insoluble drug (defined as having water solubility of less than 100 μg/mL) to demonstrate our strategy for hydrophobic drug delivery. CFZ has an extremely low (0.2 μg/mL) water solubility. The motivation for improving the delivery of CFZ lies in the fact that it has good efficacy against multidrug-resistant Tuberculosis (TB).[49–52] TB is a serious contagious disease caused by the bacterium *Mycobacterium tuberculosis* (*M. tuberculosis*) and has becoming a global health problem; in 2016, there were approximately 10.4 million new TB cases and 1.3 million TB deaths worldwide.[53] However, the extremely low water solubility of CFZ complicates its delivery by nanoparticles or other novel approaches *e.g. via* inhalation.

Herein, we developed a facile "chaperone-assisted" delivery strategy which improves the loading of CFZ and delivers a large amount of CFZ with MSNs into an aqueous environment (Figure 1). First, we found acetophenone (AP) is the most promising chaperon among 9 candidate molecules tested. Then, we compared the efficacy of AP and DMSO as non-aqueous solvents for CFZ loading and release. Next, we measured the effect of CFZ loading concentration on CFZ release and AP release and determined the optimized CFZ loading concentration. The effect of the location of AP relative to MSNs on CFZ was also explored. Finally, using the optimized AP/CFZ loaded MSNs, we investigated the antibacterial effect of this hydrotropy-based delivery strategy on intracellular *M. tuberculosis* to further validate their potential use in medicine and biomedical research. To the best of our knowledge, this is the first work to demonstrate appropriate chaperone for CFZ and to apply the strategy to the construction of nanoparticles with enhanced CFZ loading and release efficiency.

2. Experimental section

2.1 Materials

Hexadecyltrimethylammonium bromide (CTAB, 99+%), tetraethyl orthosilicate (TEOS, 98%), clofazimine (CFZ, 98+%), acetophenone (AP, 99%), 2-heptanone (98%), 2-hydroxyacetophenone (98%), sodium benzoate (99%), pyradinamide (97.5+%), nicotinamide (99.5+%), isoniazid (99+%), hexanoic acid (99+%), benzoic acid (99.5+%), sodium hydroxide (NaOH) (97+%), 4-(2-hydroxyethyl)-1-piperazineethanesulfonic acid (HEPES, 99.5+%), and ammonium nitrate (NH_4NO_3, 98+%) were purchased from Sigma-Aldrich. Dimethyl sulfoxide (DMSO, 99.9+%) was purchased from Fisher Chemical. Absolute ethanol (200 proof) was purchased from Decon Labs, Inc. All chemicals were used without further purification.

2.2 Characterization

The size and morphology of mesoporous silica nanoparticles (MSNs) were investigated by transmission electron microscopy (TEM, Tecnai T12). MSNs were dispersed in ethanol at a very low concentration (0.2 mg/mL). Ten microliters of the suspension were dropped onto the carbon-coated copper grid and dried at room temperature. The N_2 adsorption-desorption isotherms of MSNs were obtained at liquid N_2 temperature (77K) on a Autosorb-iQ (Quantachrome Instruments) apparatus. MSNs were degassed at 110 °C for 12 h before the measurement. The surface area and pore size distribution of MSNs were determined by Brunauer-Emmett-Teller (BET) and Barrett-Joyner-Halenda (BJH) methods. The dynamic light scattering (DLS) size and zeta potential value of MSNs were examined by a laser particle analyzer LPA-3100 at room temperature. The loading capacity, release capacity, and release efficiency of CFZ or AP were determined by UV-Vis Spectroscopy (Cary 5000). The absorbance of the peaks was used for quantification by Beer-Lambert Law.

2.3 Synthesis of mesoporous silica nanoparticles (MSNs)

CTAB (250 mg) was dissolved in a mixture of deionized water (120 mL) and 2 M NaOH (875 μL) under vigorous stirring. The solution was heated to 80 °C and tetraethyl orthosilicate (TEOS) (1.25 mL) was then added dropwise to the solution for about 20 seconds. The reaction was kept at 80 °C for 2 h. Subsequently, the solution was cooled to room temperature and MSNs were centrifuged and washed 3 times with ethanol. MSNs were then dispersed in 100 mL of ethanol containing 2 g of NH_4NO_3 and the reaction was refluxed for 1 h to remove the surfactant. The surfactant removal procedures were repeated twice and MSNs were washed thoroughly with ethanol and D.I. water to obtain the surfactant-free MSNs.

2.4 Screening of possible hydrotropes for CFZ

Nine different small molecules – nicotinamide, sodium benzoate, pyradinamide, isoniazid, 2-hydroxyacetophenone, benzoic acid, hexanoic acid, 2-heptanone, and acetophenone – were screened to investigate their hydrotropic ability for CFZ in H_2O. For the control lacking a hydrotrope, 1 μmol of CFZ and 1 mL of H_2O were added into a 20 mL of glass vial and sonicated for 10 min to suspend CFZ in H_2O. The undissolved CFZ was removed by centrifugation at 14000 rpm for 15 min. Then, the supernatant was collected and measured by UV-Vis spectroscopy. For experimental samples with hydrotropes, 1 μmol of CFZ, 1 mL of H_2O, and the respective hydrotrope [sodium benzoate (50 μmol, 500 μmol, or 1 mmol), pyrazinamide (50 μmol, 500 μmol, or 906 μmol), nicotinamide (50 μmol, 500 μmol, or 1 mmol), isoniazid (50 μmol, 500 μmol, 1 mmol), 2-hydroxyacetophenone (50 μmol), hexanoic acid (50 μmol), benzoic acid (28 μmol), 2-heptanone (38 μmol), or acetophenone (50 μmol)] were added into 20 mL glass vials and sonicated for 10 min. The undissolved CFZ was removed by centrifugation as described above. Finally, the supernatant was collected and measured by UV-

Vis spectroscopy. The solubility enhancement was determined by the change in absorbance at 490 nm.

2.5 Concentration dependent hydrotropy effect of AP

To investigate the hydrotropic effect of AP in more detail, we prepared concentrations ranging from 0 to 60 mM of AP in H_2O to dissolve CFZ. Similarly, 1 μmol of CFZ, 1 mL of H_2O, and the respective concentration of AP were added into 20 mL glass vials and sonicated for 10 min. The undissolved CFZ was removed by centrifugation as described above. The solubility enhancement was determined by the change in absorbance at 490 nm.

2.6 Creation of calibration curve of CFZ in AP, CFZ in ethanol-water mixture, and AP in ethanol-water mixture

To determine the loading capacity, release efficiency, and release capacity of CFZ, the calibration curves were created by dissolving CFZ in AP. The concentration of CFZ in AP ranged from 0 to 50 μM. The absorption spectra of the solutions were measured by UV-Vis spectroscopy, and the absorbance maximum (490 nm for CFZ and 244 nm for AP) was used to plot the calibration curve. The calibration curves ranging from 0 to 25 μM of CFZ dissolved in a mixture of ethanol and HEPES buffer solution (10 mM, pH = 7.4) (v/v = 1/1) were also generated. To determine the release capacity and release efficiency of AP, the calibration curve of AP was generated by dissolving AP in a mixture of ethanol and HEPES buffer solution (10 mM, pH = 7.4) (v/v = 1/1). The concentration of AP ranged from 0.25 to 66 μM.

2.7 Loading capacity analysis of clofazimine (CFZ)

The loading of CFZ was studied using DMSO or AP as loading solvents. In general, 10 mg of MSNs were dispersed in AP or DMSO with 0.1, 1, 10, or 50 mM CFZ, respectively. After 24 h stirring, the CFZ loaded MSNs were centrifuged at 14000 rpm for 10 min and the pellets were

washed three times with H_2O under sonication to remove the excess CFZ. Then, the CFZ loaded MSNs with AP or DMSO were washed with AP or DMSO, respectively, and pelleted by centrifugation. The washing steps were repeated several times until the supernatant was clear. The supernatants were collected and measured by UV-Vis spectroscopy. The loading capacity of CFZ was calculated using the maximum absorbance at 490 nm based on Beer's law, its calibration curve, and the following definition of loading capacity: (mass of loaded CFZ / mass of MSNs) x 100%.

2.8 Release of CFZ and AP in HEPES buffer

The release of CFZ and AP from MSNs was carried out in HEPES buffer solution (pH = 7.4, 10 mM). In general, 10 mg of MSNs loaded with 0.1, 1, 10, or 50 mM CFZ in AP were dispersed in 1 mL of HEPES buffer solution and stirred for 1, 2, 3, or 5 days, respectively. Afterwards, the CFZ loaded MSNs were spun down at 14000 rpm for 10 min. The supernatant was collected and mixed homogeneously with ethanol, which was then diluted and measured by UV-Vis spectroscopy. The release efficiency of CFZ and AP were calculated using their maximum absorbance at 490 nm and 244 nm, respectively, based on Beer's law, their calibration curves, and the definition of release efficiency: (mass of released CFZ / mass of loaded CFZ) x 100%.

2.9 Release of CFZ in HEPES buffer with addition of AP

To gain insight into whether the AP residing outside of the pores of MSNs would affect CFZ release, we added AP into the release buffer. After MSNs were loaded with 1 mM CFZ in DMSO, 10 mg of MSNs were dispersed in 1 mL of HEPES buffer (10 mM, pH = 7.4) with the addition of 10 μL of AP. The solution was stirred for 24 h and then centrifuged at 14000 rpm for 10 min. The supernatant was collected and measured by UV-Vis spectroscopy; the pellet of CFZ loaded MSNs was resuspended by sonication in 1 mL of HEPES buffer with the addition of 10

μL of AP and stirred for another 24 h. Again, the supernatant was collected as described above and measured by UV-Vis spectroscopy. The same procedures were repeated and the supernatant was collected and analyzed at 72 h and 120 h as described above.

2.10 Assay for killing of *M. tuberculosis* in macrophages

Human monocytic THP-1 cells (ATCC TIB202) were maintained in RPMI-1640 supplemented with 10% fetal bovine serum, GlutaMAX, and Penicillin-Streptomycin (100 IU-100 μg/mL). Prior to infection, the cells were treated with phorbol 12-myristate 13-acetate (PMA) for 3 days to differentiate them into macrophage-like cells. *M. tuberculosis* virulent strain Erdman (ATCC 35801) was cultured on Middlebrook 7H11 plates for 10 days. Lawns of bacteria were scraped from the plates, suspended in RPMI with 20 mM HEPES, and a single bacterial suspension was prepared by sonication and repeated centrifugation to remove bacterial clumps. After opsonization with human serum type AB containing active complement, the bacteria were used to infect PMA-differentiated THP-1 macrophages at a multiplicity of infection of 1:1 (bacterium:macrophage). The bacteria were incubated with macrophages for 1 hour at 37 °C, after which MSNs loaded with AP (AP-MSN), MSNs loaded with 10 mM CFZ in AP hydrotrope (AP/CFZ-MSN), or free CFZ were added to the culture of the *M. tuberculosis* infected macrophages. The concentrations of AP-MSN were 11 and 22 μg/mL. The concentrations of AP/CFZ-MSN were 5.5, 11, and 22 μg/mL, corresponding to 0.5, 1, and 2 μg/mL of CFZ, respectively. Free CFZ was dissolved in DMSO first, and then added to *M. tuberculosis* infected macrophages at concentrations of 0.5, 1, and 2 μg/mL, those concentrations of free CFZ had 0.005%, 0.01%, and 0.02% DMSO, respectively. The cells were incubated for 4 days at 37 °C, 5% CO_2-95% air, lysed with 0.1% SDS, serially diluted in Middlebrook 7H9 broth supplemented with ADC enrichment and 0.05% Tween 80, and plated on Middlebrook

7H11 agar plates. The number of bacterial colonies on the plates was enumerated after incubation for 2.5 weeks at 37 °C, 5% CO_2-95% air.[32,54]

3. Results and Discussion

3.1 Synthesis and characterization of mesoporous silica nanoparticles (MSNs)

MSNs were synthesized by a sol-gel synthetic strategy in the presence of cationic surfactant template.[15,55] By transmission electron microscopy (TEM) (Figure 2a), MSNs have a well-ordered hexagonal mesoporous structure and the average size is 100 nm in diameter. The diameter of MSNs measured by dynamic light scattering (DLS) is 165.7 nm (Figure 2b), which implies that MSNs are well-suspended in deionized (D.I.) H_2O. The zeta potential value of MSNs is –21.2 mV in D.I. H_2O. Nitrogen adsorption/desorption isotherms of MSNs were measured at 77 K. The surface area, pore volume, and pore size are 1060 m^2/g, 1.12 cm^3/g, and 2.8 nm, respectively (Figure 2c and 2d). The high surface area, characteristic of MSNs,[8,18] provides an advantage for loading cargos such as clofazimine (CFZ) and acetophenone (AP).

3.2 Clofazimine solubility enhancement

To enhance the water solubility of CFZ, we applied the concept of "hydrotropy" to the MSNs platform. During the past decades, the successful application of hydrotropy to the delivery of hydrophobic drugs by nanocarriers has been demonstrated by several research groups. For instance, Koo *et al.* used hydrotropic oligomer-conjugated glycol chitosan nanoparticles for paclitacxel (PTX) delivery.[56] Wang, *et al.* used 70 nm hydrotropic polymer-based nanocarriers to load and deliver PTX in *in vitro* studies.[57] Most of their work involved anticancer drugs, especially PTX, whose water solubility is 5.6 μg/mL.[40,58,59] To the best of our knowledge, no application of hydrotropy to the delivery of water-insoluble antibiotics from nanocarriers has been demonstrated.

It is known that highly effective hydrotropes frequently have either a phenyl ring or pyridine in their structures.[59,60] For example, sodium benzoate and nicotinamide, with either a phenyl ring or pyridine in their structures, are effective hydrotropes for PTX.[60] Therefore, sodium benzoate, nicotinamide, and other molecules with similar structures, including isoniazid, pyrazinamide, 2-hydroxyacetophenone, benzoic acid, and AP were considered candidates for hydrotropes to enhance the water solubility of CFZ. Figure 3 shows the solubility enhancement of CFZ in H_2O in the presence of the various hydrotropes mentioned above. The solubility of CFZ was determined from UV-Vis spectra where the maximum absorbance is at 490 nm. It is surprising that neither sodium benzoate nor nicotinamide is a good hydrotrope; compared with the control, the CFZ solubility enhancement is only 1.3-and 1.5-fold in 1 M of sodium benzoate and nicotinamide solution, respectively. The results indicate that isoniazid and pyrazinamide are also not effective hydrotropes for CFZ (1.7-fold in 1 M isoniazid and 1.4-fold in 1 M pyrazinamide solution). The poor hydrotropic performance of these four molecules may due to their relatively high water solubility (629 mg/mL for sodium benzoate, 500 mg/mL for nicotinamide, 140 mg/mL for isoniazid, and 50 mg/mL for pyrazinamide) as shown in Table S1. It is very difficult to provide the hydrophobic interaction between the possible hydrotropes and CFZ. In this case, the strong intermolecular force of CFZ (mainly from the hydrophobic interaction of the phenyl rings of CFZ) is much stronger than the interaction between possible hydrotropes and CFZ. Such hydrophilicity of these molecules makes them unable to associate well with the hydrophobic CFZ molecules, and thus the water solubility of CFZ was only slightly enhanced effectively.

On the other hand, the water solubility enhancement of CFZ is 1.6-fold, 1.7-fold, 2.0-fold, and 2.6-fold for 2-hydroxyacetophenone, hexanoic acid, benzoic acid, and 2-heptanone

hydrotropes, respectively. Benzoic acid and 2-heptanone have better water solubility enhancement than 2-hydroxyacetophenone or hexanoic acid. This is due to the fact that the water solubility of benzoic acid and 2-heptanone – only 3.4 mg/mL and 4.3 mg/mL, respectively – is lower than that of 2-hydroxyacetophenone and hexanoic acid – 20.0 mg/mL and 10.8 mg/mL, respectively. Thus, these hydrotropes may associate better with the hydrophobic CFZ molecules and enhance the water solubility of CFZ. In addition, the presence of the phenyl rings in the structure of hydrotropes could also contribute to improvement in the water solubility of CFZ because of the hydrophobic interactions exists between the phenyl rings of the hydrotropes and hydrophobic moiety (phenyl rings) of CFZ. For example, the solubility enhancement of CFZ in the presence of benzoic acid or hexanoic acid is 2.0 or 1.7-fold, respectively. By using benzoic acid, the solubility enhancement is higher than that of hexanoic acid due to the presence of the phenyl ring in benzoic acid. Additionally, the solubility enhancement of CFZ in the presence of 2-heptanone or AP is 2.6 or 10.1-fold. By using AP as the hydrotrope, the solubility enhancement is about four times greater than that with 2-heptanone. Therefore, the phenyl ring could effectively enhance the water solubility of CFZ because either AP or benzoic acid could provide the hydrophobic interaction between their phenyl ring and the phenyl ring of CFZ.

The hydrogen bonding between water molecules and CFZ is not strong enough to solvate CFZ since the intermolecular hydrophobic interaction between the phenyl rings of CFZ is strong. Therefore, the water solubility of CFZ is low (only 0.2 μg/mL), or water-insoluble by definition. However, for AP or 2-heptanone, there exists both a hydrophobic phenyl ring or alkyl chain and a polar carbonyl group in their chemical structures. These molecules could provide both the hydrophobic interaction between the hydrophobic phenyl ring or alkyl chain of AP or 2-heptanone and the hydrophobic moiety of CFZ, and hydrogen bonding between the carbonyl

group of AP or 2-heptanone and amine hydrogen in CFZ. Therefore, the presence of carbonyl group in AP or 2-heptanone could provide stronger interaction between the possible hydrotropes and CFZ, *e.g.* the CFZ solubility enhancement is 10.1 or 2.6-fold by using AP or 2-heptanone as the hydrotrope, higher than those of benzoic acid (2.0-fold) or hexanoic acid (1.7-fold). In terms of polarity of the possible hydrotropes, a carboxylic acid group has larger polarity than a ketone. Therefore, if we compare 2-heptanone with hexanoic acid, the solubility enhancement of CFZ is 2.6 or 1.7-fold in the presence of 2-heptanone or hexanoic acid, respectively. The higher polarity of hexanoic acid has less hydrotropic effect to increase the water solubility of CFZ. This could also be proved that the solubility enhancement of CFZ is 10.1 or 2.0-fold in the presence of AP or benzoic acid, respectively, since benzoic acid has higher polarity. Based on the above observations, AP, with good association with CFZ and both a phenyl ring and a ketone in its structure, was chosen as a promising hydrotrope for CFZ in this study. The hydrotropic efficacy of AP was examined in more detail in supporting information (Figure S1).

3.3 Clofazimine loading by using different non-aqueous solvents: AP and DMSO

To realize whether AP could also facilitate the loading of CFZ in MSNs, we compared the loading amount of CFZ by using AP to that of conventional method using DMSO, a widely-used loading solvent for dissolving poorly water-soluble drugs.[2,14] We called the method of using AP the "chaperone-assisted" method due to the preferential interaction between AP and CFZ, making AP act like a chaperon carrying the CFZ with it (Figure 4a). CFZ loading into MSNs was achieved by soaking MSNs in CFZ solutions with various concentrations dissolved in AP or DMSO. After 24 h loading of CFZ, the CFZ-loaded MSNs were introduced back to aqueous solution. To calculate the loading capacity, which is defined as (the mass of loaded CFZ / the mass of MSNs) x 100%, the CFZ loaded MSNs with AP or DMSO were respectively washed

with AP or DMSO several times until the supernatant after centrifugation was clear. Those supernatants were collected and measured by UV-Vis spectroscopy. The total amount of CFZ loaded in MSNs was calculated based on Beer's law and its calibration curve (Figure S2). From Figure 4b, the loading capacity of 0.1, 1, and 10 mM CFZ by using DMSO as the loading solvent were found to be 0.2, 0.9, and 5.9 %, respectively. However, with AP as the loading solvent, the higher loading capacity were achieved under all loading concentrations of CFZ, which were 0.3, 1.3, 9.6, and 26.8 % for 0.1, 1, 10, and 50 mM CFZ, respectively. The loading capacity of CFZ increased with the loading concentration of CFZ. The higher loading capacity of CFZ by using AP as the loading solvent can be explained by two reasons: (1) the CFZ solubility in AP (>71 mg/mL) is higher than in DMSO (5 mg/mL), so that the saturated concentration of CFZ in AP (more than 150 mM) is much higher than in DMSO (only 10.5 mM); (2) DMSO is miscible with water, so most of the DMSO molecules were removed by water during the washing steps, leading to the release of some CFZ molecules from MSNs together with DMSO. However, the water solubility of AP is only 6.1 mg/mL, so a large amount of AP was still loaded in the pores of MSNs after they were re-dispersed in aqueous solution (Figure 4a). As will be shown in the next section, the AP in the pores is essential for good CFZ release.

Based on the significant enhancement of CFZ loading by AP, it was of interest to investigate the detailed relationship between the loading of AP chaperone and its cargo CFZ. MSNs were loaded with AP itself (no CFZ), or AP with 0.1, 1, 10, and 50 mM solubilized CFZ. The pore volume of MSNs is 1.12 cm^3/g; hence the maximum volume for cargo loading is 1.12 μL/mg. The density of AP is 1.03 g/cm^3, and thus the maximum loading capacity would be 115.4%. When AP itself (0 mM CFZ), or AP with 0.1, 1, 10, and 50 mM solubilized CFZ were used as the loading solvents, the loading capacity of AP was found to be 100.9 %, 102.4 %, 101.1%,

97.2 %, and 71.4 %, respectively (Figure 4c). The amount of loaded AP in MSNs corresponds to 8397.8, 8522.7, 8414.5, 8089.9, and 5942.6 nmole/mg, and the amount of loaded CFZ in MSNs was 6.3, 27.5, 202.8, and 566.1 nmole/mg at those respective CFZ loading concentrations (Table 1). This implies that when the CFZ loading capacity is low (no higher than 1.3 %, Figure 4b), regardless of the presence of CFZ, about 88% of the pore volume of MSNs is filled with AP after loading, which is reasonable since the low water solubility of AP (only 6.1 mg/mL) makes a large amount of AP remain in the pores of MSNs after they are re-dispersed in aqueous solution. The loading capacity of AP is lower at higher CFZ concentrations (10 and 50 mM), at which the loading capacity of CFZ was enhanced (9.6 % and 26.8 %, Figure 4b). This is because part of the pore volume of MSNs is occupied by CFZ, thus reducing the volume available for AP loading. The mole ratios of AP to CFZ loaded in MSNs with those CFZ loading concentrations was calculated to be 1352.8, 306.0, 39.9, and 10.5, respectively (Table 1). As CFZ loading concentrations in AP increase, both the amount of loaded CFZ and the mole ratio of CFZ to AP increase.

3.4 Clofazimine release to aqueous solution by using different non-aqueous solvents: AP and DMSO

Before applying the methods with AP and DMSO to deliver CFZ to biological systems, we examined their capability for facilitating the release of CFZ into aqueous solution. MSNs loaded with CFZ (1 mM) either by DMSO or AP were dispersed in HEPES buffer solution (pH = 7.4) for 1, 2, 3, or 5 days, respectively (Figure 4a). Figure S3a shows the UV-Vis spectra of the supernatant after CFZ released from MSNs in buffer solution with DMSO as the loading solvent. The absorption peak of CFZ at 490 nm is not evident, indicating that the release of CFZ is negligible even after 5 days. This phenomenon could be explained as a result of the water-

insoluble property of CFZ, making the drug molecules themselves prefer to stay in the pores of MSNs. On the contrary, with AP as the loading solvent, the release of CFZ could be easily found in the UV-Vis spectra with the apparent peaks at 490 nm (Figure S3b). The absorbance peaks at 490 nm increased with time between 5 days, and the absorbance is significantly different from those with DMSO. To quantify the release amount of CFZ, the time dependent release efficiency of CFZ using either DMSO or AP was calculated (Figure 4d) based on Beer's law and its calibration curve (Figure S4). The release efficiency is defined as (the mass of released CFZ / the mass of loaded CFZ) x 100%. By using the "chaperone-assisted" strategy with AP, the release efficiency of CFZ achieved 47.2%, which is 2300 times higher than that by the conventional method with DMSO (0.02%) (Figure 4d). This significant enhancement in the release efficiency of CFZ by AP could also be clearly observed in the photograph of the supernatant (Figure 4e).

3.5 Effect of clofazimine loading concentration on clofazimine release

To optimize the release of CFZ in aqueous environment using the "chaperone-assisted" delivery strategy, we explored the effect of CFZ loading concentration on the long-term release behavior of CFZ. The release of CFZ was confirmed by the absorbance peaks at 490 nm in the UV-Vis spectra measured from the supernatants collected after spinning down MSNs after 1, 2, 3, and 5 days (Figure S3b). The time-dependent release capacity of CFZ was calculated based on Beer's law and its calibration curve (Figure S4). Release capacity is defined as: (the mass of released CFZ / the mass of MSNs) x 100%. Figure 5a shows the time-dependent release capacitiy of CFZ in HEPES buffer solution (pH = 7.4) with four different CFZ loading concentrations (0.1, 1, 10, and 50 mM) in AP. The absorbance peaks increase with time up to 5 days. Regardless of the CFZ loading concentration, the amount of CFZ released gradually increases with time, until it levels off at about five days. The amount of CFZ released from

MSNs loaded with 0.1 mM CFZ in AP is only 0.10 % on day 5, which is mainly due to the tiny amount of CFZ (0.3 % loading capacity) loaded in MSNs. For the MSNs loaded with 1 and 10 mM CFZ in AP, the CFZ release capacity on day 5 was 0.56 % and 0.54 %, respectively. Even though the amount of CFZ loaded with those two samples (1.3 % and 9.6 % CFZ loading capacity, respectively) differed by 7-fold, the amount of CFZ released was nearly the same. However, the CFZ release capacity of the MSNs loaded with 50 mM CFZ in AP on day 5 is only 0.27 %, lower than those loaded with 1 and 10 mM CFZ in AP. This low CFZ release capacity at this high CFZ loading concentration may be due to a small amount of AP in the pores of MSNs that contain a large amount of CFZ (26.8 % CFZ loading capacity) as referred to Table 1, which shows the mole ratio of AP/CFZ to be only 10.5. This less amount of AP renders the environment inside the pores much more hydrophobic and thus reducing the "chaperone-assisted" effect or the hydrotropic effect. The time-dependent release efficiency of CFZ with four different CFZ loading concentrations (0.1, 1, 10, and 50 mM) was also calculated (Figure 5b). Release efficiency is defined as: (the mass of released CFZ / the mass of loaded CFZ in MSNs) x 100%. The time-dependent release efficiency on day 5 for MSNs loaded with 0.1, 1, 10, and 50 mM CFZ in AP is 42.3 %, 47.2 %, 4.6 %, and 0.1%, respectively. The lowest release efficiency, observed when MSNs were loaded with 50 mM CFZ in AP, indicates that most of the loaded CFZ remains in the pores of MSNs, which again may be due to the small amount of loaded AP and the enhanced hydrophobicity in the pores of MSNs as described above.

3.6 Effect of clofazimine loading concentration on acetophenone release

After the "chaperone-assisted" strategy was successfully demonstrated, we studied the effect of CFZ cargo loading concentration on the release of AP chaperone (Figure 5c and 5d). The release efficiency of AP was calculated based on Beer's law and its calibration curve (Figure

S5). The time-dependent release capacity of AP from MSNs loaded with 0.1, 1, 10, and 50 mM CFZ in AP is lower than from MSNs not loaded with CFZ on day 1 (Figure 5c). Nevertheless, the release capacity of AP from MSNs loaded with CFZ substantially increases on day 2. Finally, the release capacity of AP on day 5 reaches 94.2, 90.0, 77.8, and 53.6 % from MSNs loaded with 0.1, 1, 10, and 50 mM CFZ in AP, respectively. For the release efficiency of AP from MSNs loaded with 0.1, 1, 10, and 50 mM CFZ, only 22, 11, 12, and 13 % were found on day 1, much lower than without loaded CFZ (33%) (Figure 5d). However, on day 2, the release efficiency of AP from MSNs loaded with 0.1, 1, 10, and 50 mM CFZ in AP achieves 60, 61, 59, and 57 %, respectively, which is close to that without loaded CFZ (58%). Finally, on day 5, the release efficiency of AP reaches about 92, 89, 80, and 75 % for MSNs loaded with 0.1, 1, 10, and 50 mM CFZ in AP, respectively, and reaches about 95% for the MSNs loaded with AP itself (0 mM CFZ). Interestingly, the result on day 5 shows that the release efficiency of AP decreases as the loading concentration of CFZ increases. This finding together with the lower loading capacity of AP at 10 and 50 mM CFZ loading concentration (Figure 4c) adequately explain the much lower release capacity of AP when MSNs are loaded with 10 mM or 50 mM CFZ than when MSNs are loaded with AP without any CFZ (95.9%) (Figure 5c).

The sigmoidal release profiles of both CFZ and AP loaded in MSNs are characterized by slow release during the first day followed by increased release at later time points, and a final leveling off (Figure 5b and 5d). In the presence of both CFZ and AP in MSNs, almost all of the CFZ (Figure 5b) as well as the greater part of AP (Figure 5d) remain inside the pores on day 1, especially for the MSNs loaded with 1, 10, and 50 mM CFZ in AP. This supports that there may exist an interaction between CFZ and AP in the pores of MSNs, and that this association favors most of the AP molecules residing in the pores of MSNs, reducing the AP release on day 1. The

loaded CFZ molecules may sterically block the release of AP from MSNs as well. The better AP release compared to that of CFZ on day 1 could be explained by the higher water solubility of AP than CFZ, so that the release of AP in aqueous environment can occur in a short period of time. For MSNs loaded with 0.1 and 1 mM CFZ in AP, the release efficiency of AP increases significantly after day 1 (Figure 5d), which corresponds to the substantial increase in CFZ release efficiency on day 2 (Figure 5b). This feature is due to the high mole ratio of AP/CFZ in the pores of MSNs with 0.1 and 1 mM CFZ (Table 1). The abundant AP chaperone in the pores carry CFZ out of MSNs and thus facilitates CFZ release into an aqueous environment. Interestingly, for particles loaded with 10 and 50 mM CFZ, the CFZ release efficiency shows no significant increase during those five days compared with the dramatic increase in AP release efficiency after day 1. This is because the mole ratio of AP/CFZ is low at those CFZ loading concentrations (Table 1), and thus the interaction between AP and CFZ is not strong enough to carry CFZ out of MSNs and into the aqueous environment. In other words, when the mole ratio of AP/CFZ is low, even though the interaction between CFZ and AP in the pores retards the release of AP, the high water solubility of AP dominates such that more AP is released into an aqueous environment as the release time increases.

The "chaperone-assisted" delivery strategy makes use of the interaction between CFZ cargo and AP chaperon which provides the mechanism for the release of CFZ from MSNs, and thus significantly enhances the water solubility of CFZ. By carefully tuning the mole ratio of AP/CFZ, we can control the dosage and the release profile of CFZ over time. This would be favorable in terms of improving the bioavailability and the efficacy of CFZ, as well as reducing the side-effect causing by the overdose of CFZ.

3.7 Effect of external acetophenone on clofazimine release

As the chaperon, AP is supposed to be stayed together with its CFZ cargo in the pores of MSNs to bring its assistance into full play. To further confirm the idea of "chaperone-assisted" delivery, we studied the release of CFZ in a buffer solution with or without the addition of dissolved AP. Instead of using AP as the loading solvent, DMSO was used for loading CFZ to prevent AP from being present in the pores of MSNs. Release buffer with or without the addition of AP was used for CFZ release. With DMSO as the loading solution, the release efficiency of CFZ released in HEPES buffer solution (10 mM, pH = 7.4) without the addition of AP is only 0.02% after 120 h, which indicates that almost all of the CFZ stays in the pores of MSNs (Figure 6). The release efficiency of CFZ released in HEPES buffer solution with the addition of AP, on the other hand, is only 4.3% after 120 h. Both of these CFZ release efficiencies are significantly lower than that with AP as the loading solvent and HEPES buffer solution as the release buffer (47.2%). This result suggests that the CFZ release efficiency is significantly enhanced by the AP loaded inside the pores of MSNs together with CFZ, of which the interaction between CFZ cargo and AP chaperon inside the pores contributes substantially to the significant improvement of CFZ release. On the other hand, AP outside of the MSNs that doesn't have good interaction with CFZ only contributes to about 1/10th of the CFZ release. This slightly greater CFZ release could be explained by the increased hydrophobicity of the environment causing by the AP located in solution outside of MSNs. This study further strengthens the idea of "chaperone-assisted" delivery, where MSNs act like a primary vehicle carrying both a secondary vehicle – the AP chaperon – and the CFZ cargo inside. As the chaperon, AP carries the CFZ and brings it out and away from MSNs effectively.

3.8 Antibacterial effect of acetophenone-assisted clofazimine delivery by MSNs

To explore the antibacterial effect of the developed "chaperone-assisted" delivery strategy shown in Figure 7a, we examined the treatment efficacy of the CFZ loaded MSNs using a macrophage model of *Mycobacterium tuberculosis (M. tuberculosis)* infection. The mole ratio of AP/CFZ was tuned and the optimized CFZ loading concentration was found to be 10 mM considering both the loading capacity and release capacity of CFZ (Figure 4b and 5a). The *M. tuberculosis*-infected macrophages were treated with MSNs loaded with 10 mM CFZ in AP (AP/CFZ-MSN) for 4 days (Figure 7a). As controls, the macrophages were untreated or treated with MSNs loaded with AP only (AP-MSN), or with free CFZ dissolved in a mixture of DMSO and H_2O (CFZ/DMSO). All of the infected macrophages were lysed at day 4 post-infection and the lysates were plated for viable *M. tuberculosis*. The number of *M. tuberculosis* colony forming units (CFUs) recovered from the macrophages was enumerated to determine bacterial viability under each treatment. As shown in Figure 7b, treatment with AP-MSN (11 and 22 μg/mL) for 4 days without CFZ had little effect on *M. tuberculosis* because the number of bacteria in macrophage monolayers (6.29, and 6.25 log CFU, respectively) was similar to and not statistically different from the number in untreated macrophages (6.51 log CFU). In contrast, AP/CFZ-MSN killed the intracellular bacteria in a dose-dependent manner. AP/CFZ-MSN at concentrations of 5.5, 11, and 22 μg/mL correspond to 0.5, 1, and 2 μg/mL of free CFZ dissolved in DMSO. The number of viable bacteria after treatment with those concentrations of AP/CFZ-MSN was 5.97, 5.82, and 5.50 log CFU, respectively, suggesting that 90% of bacteria was killed (the number of bacteria decreased by 1 log CFU) in macrophages treated with 22 μg/mL of AP/CFZ-MSN. We also compared the effect of free CFZ with that of the MSN-encapsulated CFZ. The treatment efficacy of AP/CFZ-MSN dispersed in culture medium was similar to that of an equivalent amount of CFZ dissolved in the mixture of DMSO and culture

medium without MSNs. This comparison shows that with the help of the AP chaperon, most of the CFZ loaded inside MSNs is efficiently released in the macrophages and kill the bacteria effectively and selectively (Figure 7a).

To investigate if the "chaperone-assisted" delivery strategy with AP, an FDA approved food additive, has any cytotoxicity to the macrophages, we examined the viability of the infected macrophages after the treatment with AP-MSN and AP/CFZ-MSN for 4 days. No significant decrease in macrophage viability was detected (Figure 7c) at the concentrations studied. No adverse effect on the morphological appearance of the macrophages treated with AP-MSN or AP/CFZ-MSN was observed. Taken together, these results show that the "chaperone-assisted" CFZ delivery strategy *via* MSNs has no evident toxicity to macrophages but can selectively and efficiently kill the bacteria residing inside them due to the significant release of CFZ from MSNs.

4. Conclusions

In this study, we have developed a novel "chaperone-assisted" strategy based on mesoporous silica nanoparticles (MSNs) to both load water-insoluble drugs into MSN carriers and release them into aqueous biological environment. First, we utilized the concept of "hydrotropy" to explore the nine candidate small molecules for their utility to enhance the water solubility of a water-insoluble antibiotics — clofazimine (CFZ), who has good efficacy against multidrug-resistant Tuberculosis (TB). Acetophenone (AP) was selected as the most efficacious solvent to enhance 10.1-fold of the water solubility of CFZ. Acting as a chaperon, AP not only brought a great amount of CFZ cargos (26.8% loading capacity of CFZ) into the MSN nanocarrier, but carried a significant amount of CFZ cargos (47.2% release efficiency of CFZ) out from MSNs into the aqueous solution. This release efficiency of CFZ achieved is 2300 times

higher than that by conventional method using DMSO (0.02%). This considerable increase in CFZ release is mainly driven by the release of AP chaperon from the chaperon-rich pores of MSNs, which allows CFZ cargo to be carried together into the aqueous solution, and can be supported by our three findings: (1) a lower loading concentration of CFZ (1 mM) gave a higher release efficiency of CFZ (47.2%) compared with a higher loading concentration of CFZ (0.1%); (2) AP in the solution outside of MSNs only minimally increased the release efficiency of CFZ (4.3%); (3) without AP, the release efficiency of CFZ was only 0.02%. We examined this delivery strategy in a macrophage model of *Mycobacterium tuberculosis (M. tuberculosis)* infection using MSNs loaded with the optimized ratio of CFZ and AP (10 mM CFZ in AP). *M. tuberculosis* residing inside macrophages were efficiently killed (reduced by 1 log CFU) by the high amount of the released CFZ, which is comparable to that with the same amount of CFZ dissolved in a mixture of DMSO and culture medium. No adverse effect on the morphological appearance of the macrophages treated with either MSNs loaded with AP or MSNs loaded with CFZ and AP was observed. This novel "chaperone-assisted" delivery strategy for CFZ could also be applied to other hydrophobic drugs with their suitable loading solvents (chaperone), opening up opportunities to apply this drug delivery strategy for further use in medicine and biomedical research.

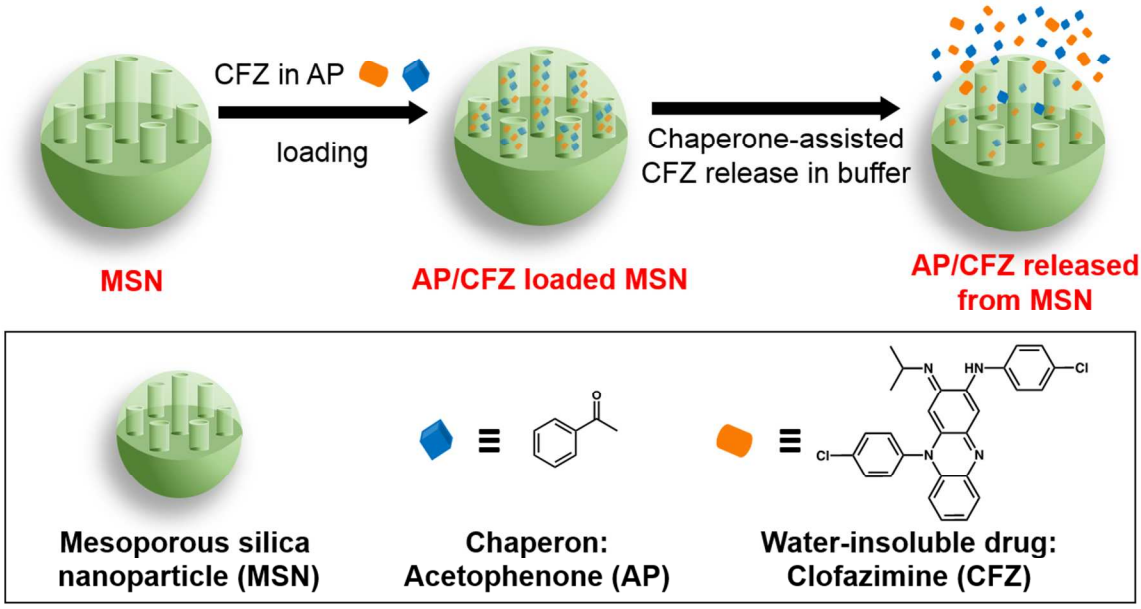

Figure 1. Chaperone-assisted delivery strategy for water-insoluble drugs. Clofazimine (CFZ) was chosen as an example of a water-insoluble antibiotic. Acetophenone (AP) acts like a chaperon bringing CFZ cargo into the vehicle — mesoporous silica nanoparticles (MSNs) and then carrying CFZ cargo out from the MSNs effectively.

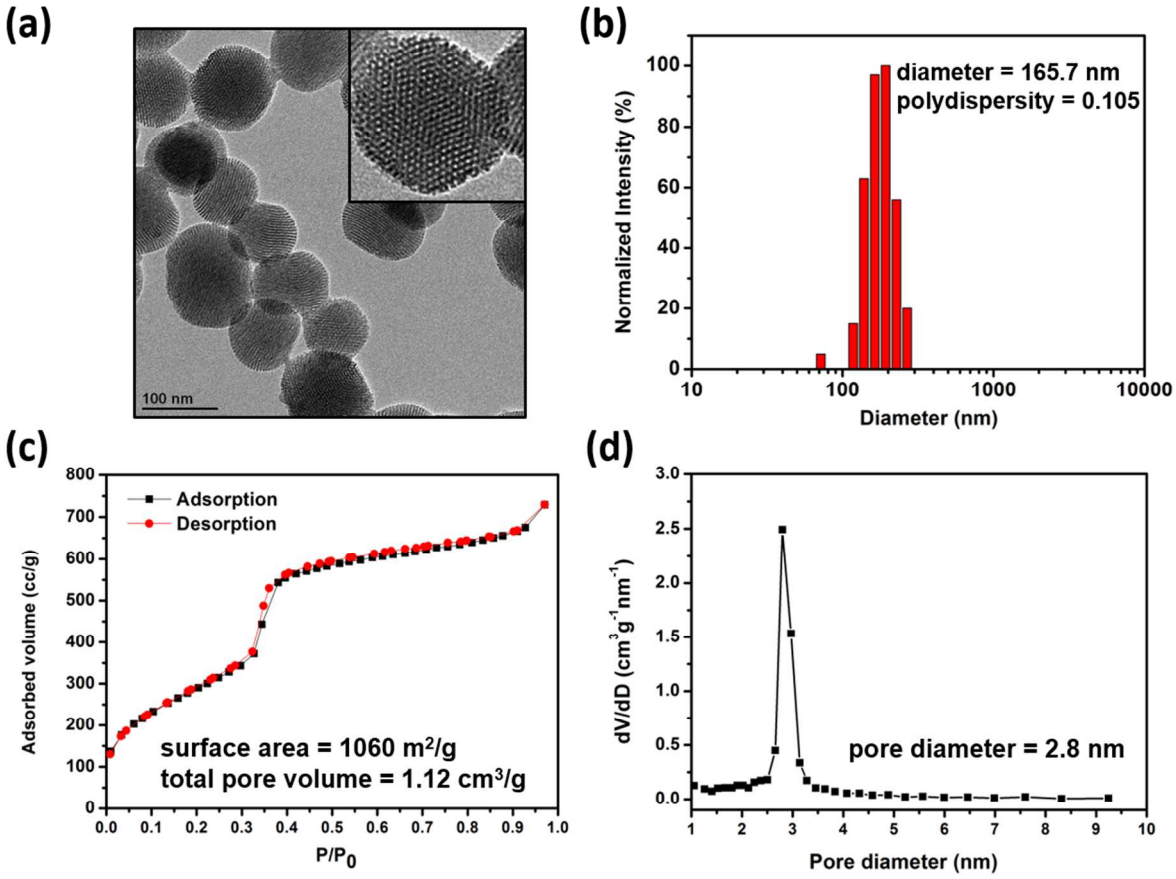

Figure 2. (a) TEM image of mesoporous silica nanoparticles (MSNs). Inset shows the enlarged image. (b) Dynamic light scattering diameter distribution of MSNs in D.I. H_2O. The diameter of the MSNs is 165.7 nm. (c) Nitrogen adsorption-desorption isotherms of MSNs at 77 K. BET surface area and pore volume are 1060 m^2/g and 1.12 cm^3/g, respectively. (d) Pore diameter distribution of MSNs. Average pore diameter of MSNs is 2.8 nm.

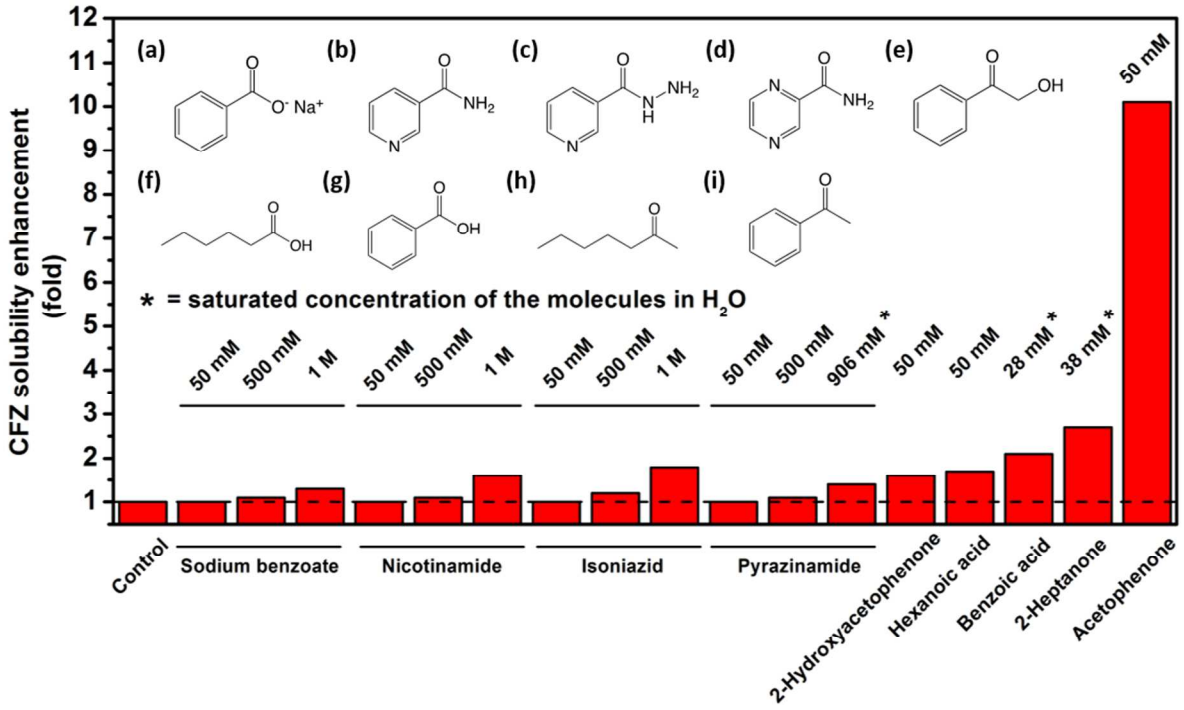

Figure 3. CFZ solubility enhancement in the presence of (a) sodium benzoate, (b) nicotinamide, (c) isoniazid, (d) pyrazinamide, (e) 2-hydroxyacetophenone, (f) hexanoic acid, (g) benzoic acid, (h) 2-heptanone, and (i) acetophenone. The solubility of CFZ in deionized water without the addition of any molecule served as a control.

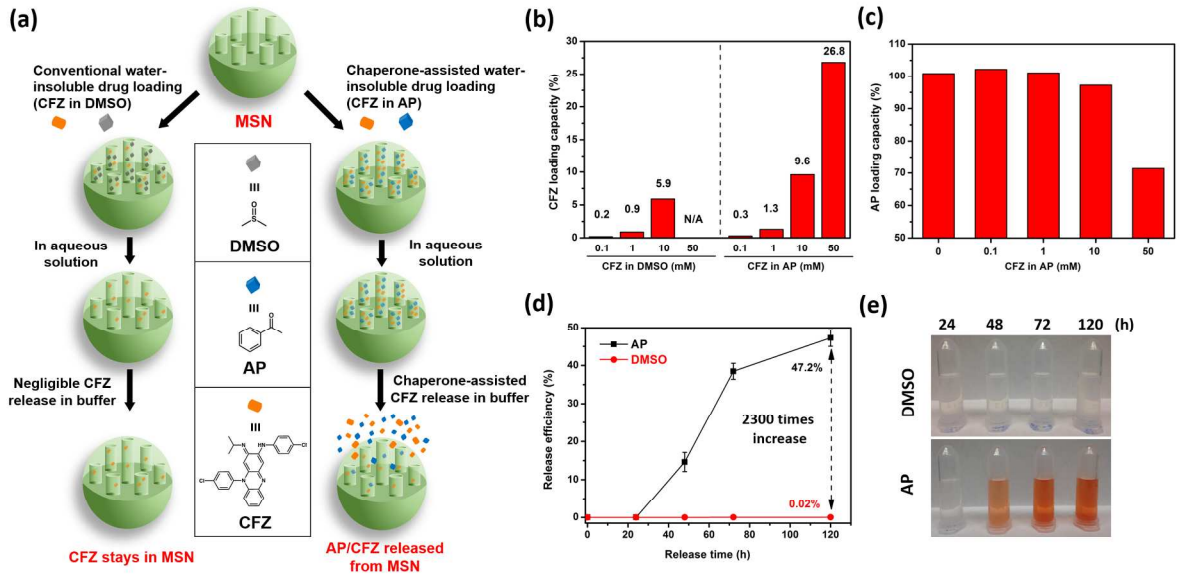

Figure 4. (a) Schematic illustration of conventional method (CFZ in DMSO) or chaperone-assisted method (CFZ in AP) for water-insoluble CFZ loading in MSN. By using AP as the chaperone, CFZ release from MSNs could be enhanced significantly. Loading capacity of (b) CFZ and (c) AP using 0.1, 1, or 10 mM CFZ in DMSO or 0, 0.1, 1, 10, or 50 mM CFZ in AP as the loading solution. The concentration of MSNs was 10 mg/mL (d) Time-dependent release efficiency of CFZ in HEPES buffer solution (10 mM, pH = 7.4) with 1 mM CFZ in DMSO or 1 mM CFZ in AP as loading solutions. (e) Photographs of supernatant after CFZ release collected at selected time points. MSNs were loaded with 1 mM CFZ in DMSO or 1 mM CFZ in AP.

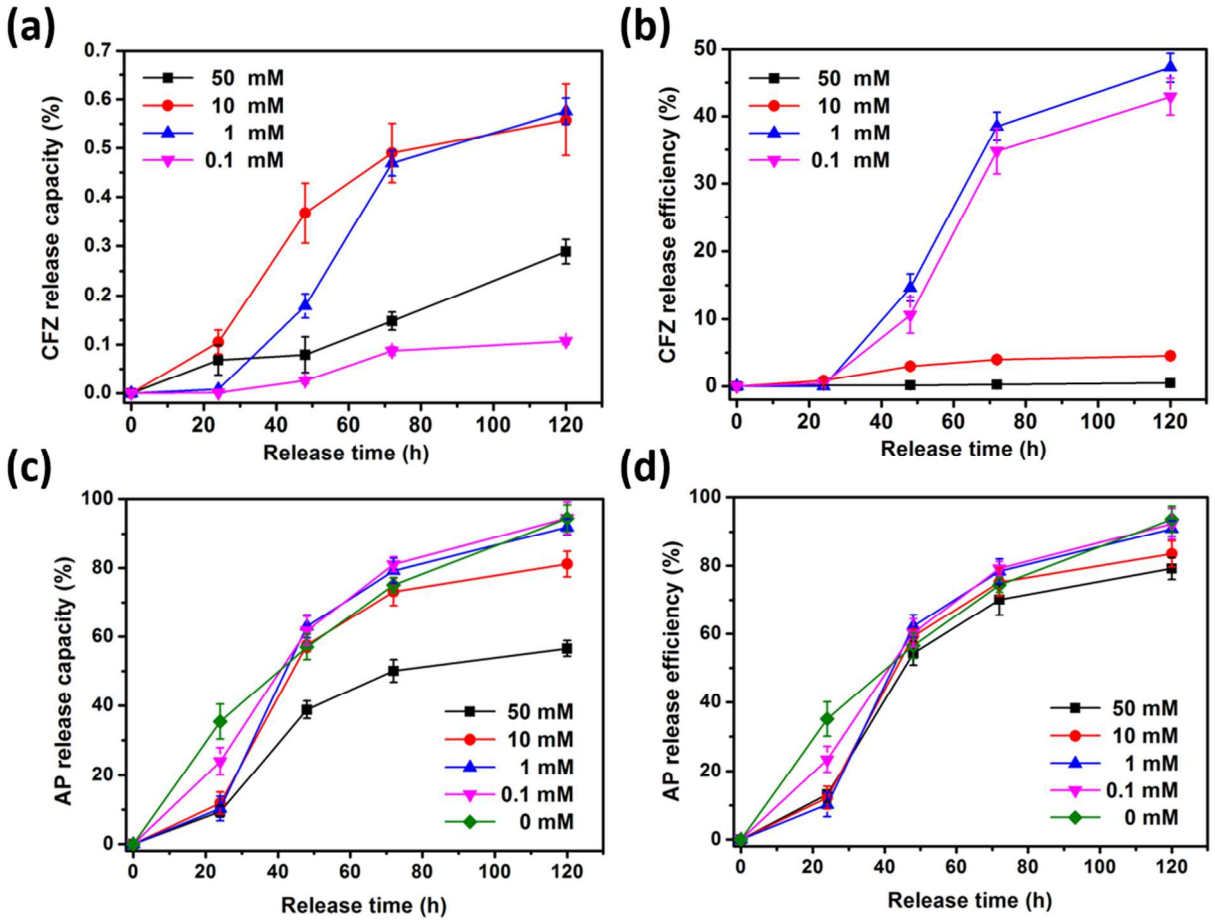

Figure 5. Time-dependent release capacity of (a) CFZ and (c) AP and release efficiency of (b) CFZ and (d) AP in HEPES buffer solution (10 mM, pH = 7.4) with 0, 0.1, 1, 10, and 50 mM CFZ in AP as loading solutions. The concentration of MSNs in both loading solution and release buffer solution was 10 mg/mL (n=3).

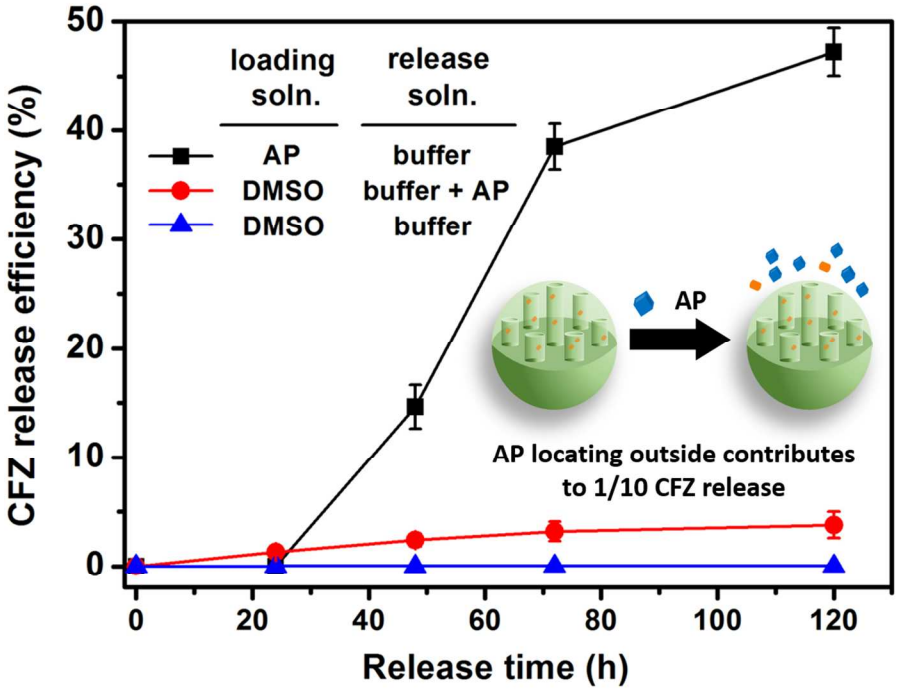

Figure 6. Time-dependent release efficiency of CFZ in HEPES buffer solution (10 mM, pH = 7.4) with or without the addition of AP to the buffer solution. After loading with 1 mM CFZ in DMSO, 10 μL of AP was added to the buffer solution (10 mg MSNs/mL, 1 mL) (n=3).

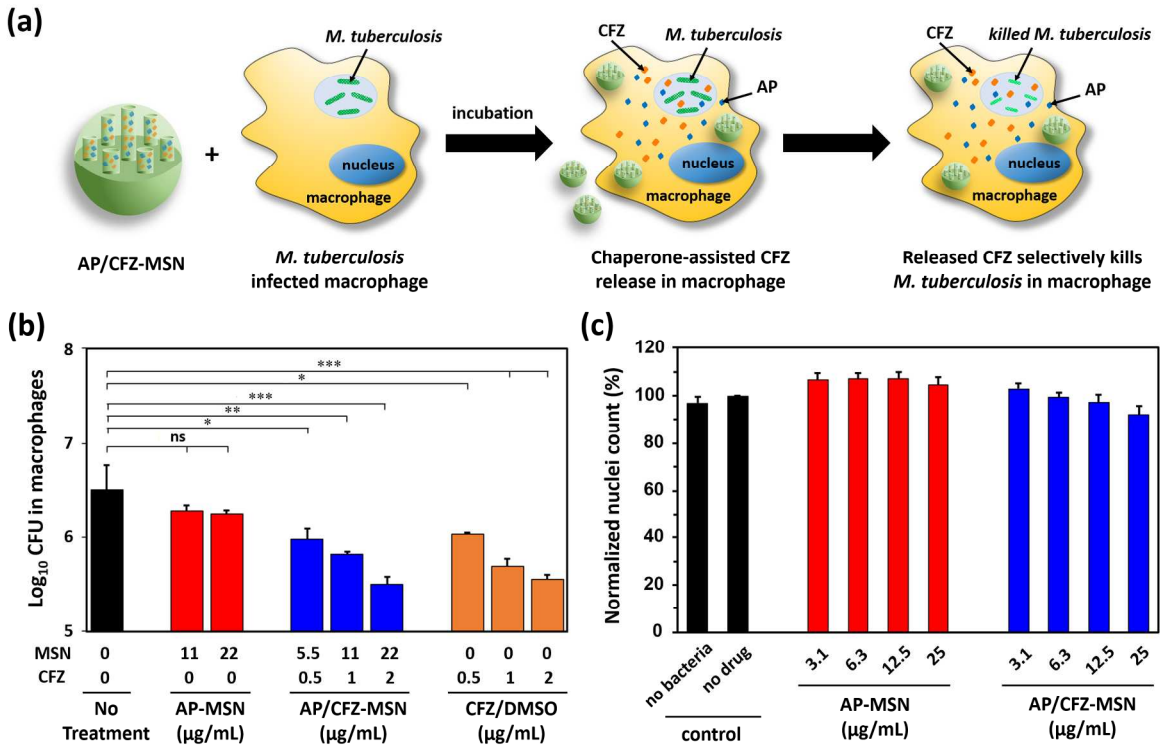

Figure 7. (a) Schematic illustration of applying chaperone-assisted CFZ delivery strategy to selectively killing *M. tuberculosis* in macrophage. (b) AP/CFZ loaded MSNs kill *M. tuberculosis in vitro* in macrophage cultures. *M. tuberculosis*-infected THP-1 macrophages were untreated, treated with MSN loaded with AP (AP-MSN), treated with MSN loaded with CFZ and AP (AP/CFZ-MSN), or treated with CFZ dissolved in a mixture of DMSO and H_2O (CFZ/DMSO) for 4 days. Bacterial colony forming units (CFUs) were determined by spreading serially diluted lysates of the infected macrophages on agar plates. CFU data are shown as the mean ± standard deviation. Statistical analysis was performed using one-way ANOVA with Tukey's correction for multiple comparisons. ns, not significant; $*p < 0.05$; $**p < 0.01$; $***p < 0.001$ (c) Count of macrophage nuclei per 10x microscopic field normalized to that of the macrophage control wells without addition of drug. Count of macrophage nuclei per microscopic field is used as a surrogate of macrophage viability, as dead macrophages detach and are lost from the monolayer

over the long incubation period. Human THP-1 macrophages were either not infected (no bacteria) or infected with *Mycobacterium tuberculosis* in the absence of nanoparticles (no drug) or in the presence of AP-MSN and AP/CFZ-MSN with serial two-fold increasing concentration ranging from 3.1 to 25 μg/mL, as indicated. At the end of a 4-day incubation, macrophages were fixed with paraformaldehyde and the nuclei were stained with DAPI and imaged with an ImageXpress High Content Screening system using a 10x objective lens. The acquired images were analyzed using the Count Nuclei module of MetaXpress software to quantitate numbers of nuclei per 10x field. Data shown are mean ± sem of three biological replicates.

Table 1. Summary of the amount of loaded CFZ and AP in MSNs (nmole/mg) and the mole ratio of AP/CFZ loaded in MSNs.

CFZ in AP (mM)	0	0.1	1	10	50
loaded CFZ/MSNs (nmole/mg)	0	6.3	27.5	202.8	566.1
loaded AP/MSNs (nmole/mg)	8397.8	8522.7	8414.5	8089.9	5942.6
mole ratio of AP/CFZ	n/a	1352.8	306.0	39.9	10.5

ASSOCIATED CONTENT

Supporting Information.

Figures S1 to S5 and Table S1 are available free of charge *via* the Internet at http://pubs.acs.org.

AUTHOR INFORMATION

Corresponding Author

*zink@chem.ucla.edu

ORCID

Wei Chen: 0000-0002-2909-3023

Chi-An Cheng: 0000-0002-6657-9137

Jeffrey I. Zink: 0000-0002-9792-4976

ACKNOWLEDGMENT

The authors gratefully acknowledge financial support by Defense Threat Reduction Agency Grant HDTRA1-13-1-0046.

NOTE

The authors declare no competing financial interest.

REFERENCES

(1) Khadka, P.; Ro, J.; Kim, H.; Kim, I.; Kim, J. T.; Kim, H.; Cho, J. M.; Yun, G.; Lee, J. Pharmaceutical Particle Technologies: An Approach to Improve Drug Solubility, Dissolution and Bioavailability. *Asian J. Pharm. Sci.* **2014**, *9*, 304–316.

(2) Ferris, D. P.; Lu, J.; Gothard, C.; Yanes, R.; Thomas, C. R.; Olsen, J. C.; Stoddart, J. F.; Tamanoi, F.; Zink, J. I. Synthesis of Biomolecule-Modified Mesoporous Silica Nanoparticles for Targeted Hydrophobic Drug Delivery to Cancer Cells. *Small* **2011**, *7*, 1816–1826.

(3) Wu, S.-H.; Mou, C.-Y.; Lin, H.-P. Synthesis of Mesoporous Silica Nanoparticles. *Chem. Soc. Rev.* **2013**, *42*, 3862–3875.

(4) Tarn, D.; Ashley, C. E.; Xue, M.; Carnes, E. C.; Zink, J. I.; Brinker, C. J. Mesoporous Silica Nanoparticle Nanocarriers: Biofunctionality and Biocompatibility. *Acc. Chem. Res.* **2013**, *46*, 792–801.

(5) Ruehle, B.; Saint-Cricq, P.; Zink, J. I. Externally Controlled Nanomachines on Mesoporous Silica Nanoparticles for Biomedical Applications. *Chemphyschem* **2016**, *17*, 1769–1779.

(6) Tang, F.; Li, L.; Chen, D. Mesoporous Silica Nanoparticles: Synthesis, Biocompatibility and Drug Delivery. *Adv. Mater.* **2012**, *24*, 1504–1534.

(7) Chou, C.-C.; Chen, W.; Hung, Y.; Mou, C.-Y. Molecular Elucidation of Biological Response to Mesoporous Silica Nanoparticles in Vitro and in Vivo. *ACS Appl. Mater. Interfaces* **2017**, *9*, 22235–22251.

(8) Li, Z.; Barnes, J. C.; Bosoy, A.; Stoddart, J. F.; Zink, J. I. Mesoporous Silica Nanoparticles in Biomedical Applications. *Chem. Soc. Rev.* **2012**, *41*, 2590–2605.

(9) Li, Y.; Shi, J. Hollow-Structured Mesoporous Materials: Chemical Synthesis, Functionalization and Applications. *Adv. Mater.* **2014**, *26*, 3176–3205.

(10) Wei, J.; Sun, Z.; Luo, W.; Li, Y.; Elzatahry, A. A.; Al-Enizi, A. M.; Deng, Y.; Zhao, D. New Insight into the Synthesis of Large-Pore Ordered Mesoporous Materials. *J. Am. Chem. Soc.* **2017**, *139*, 1706–1713.

(11) Suteewong, T.; Sai, H.; Hovden, R.; Muller, D.; Bradbury, M. S.; Gruner, S. M.; Wiesner, U. Multicompartment Mesoporous Silica Nanoparticles with Branched Shapes: An Epitaxial Growth Mechanism. *Science* **2013**, *340*, 337–341.

(12) Zhang, Q.; Wang, X.; Li, P. Z.; Nguyen, K. T.; Wang, X. J.; Luo, Z.; Zhang, H.; Tan, N. S.; Zhao, Y. Biocompatible, Uniform, and Redispersible Mesoporous Silica Nanoparticles for Cancer-Targeted Drug Delivery in Vivo. *Adv. Funct. Mater.* **2014**, *24*, 2450–2461.

(13) Argyo, C.; Weiss, V.; Bräuchle, C.; Bein, T. Multifunctional Mesoporous Silica Nanoparticles as a Universal Platform for Drug Delivery. *Chem. Mater.* **2014**, *26*, 435–451.

(14) Lu, J.; Liong, M.; Zink, J. I.; Tamanoi, F. Mesoporous Silica Nanoparticles as a Delivery System for Hydrophobic Anticancer Drugs. *Small* **2007**, *3*, 1341–1346.

(15) Ruehle, B.; Clemens, D. L.; Lee, B.-Y.; Horwitz, M. A.; Zink, J. I. A Pathogen-Specific Cargo Delivery Platform Based on Mesoporous Silica Nanoparticles. *J. Am. Chem. Soc.* **2017**, *139*, 6663–6668.

(16) Li, Z.; Clemens, D. L.; Lee, B. Y.; Dillon, B. J.; Horwitz, M. A.; Zink, J. I. Mesoporous Silica Nanoparticles with pH-Sensitive Nanovalves for Delivery of Moxifloxacin Provide Improved Treatment of Lethal Pneumonic Tularemia. *ACS Nano* **2015**, *9*, 10778–10789.

(17) Yan, H.; Teh, C.; Sreejith, S.; Zhu, L.; Kwok, A.; Fang, W.; Ma, X.; Nguyen, K. T.; Korzh, V.; Zhao, Y. Functional Mesoporous Silica Nanoparticles for Photothermal-Controlled Drug Delivery in Vivo. *Angew. Chem. Int. Ed.* **2012**, *51*, 8373–8377.

(18) Chen, W.; Tsai, P.-H.; Hung, Y.; Chiou, S.-H.; Mou, C.-Y. Nonviral Cell Labeling and Differentiation Agent for Induced Pluripotent Stem Cells Based on Mesoporous Silica Nanoparticles. *ACS Nano*, **2013**, *7*, 8423–8440.

(19) Chang, J.-H.; Tsai, P.-H.; Chen, W.; Chiou, S.-H.; Mou, C.-Y. Dual Delivery of siRNA and Plasmid DNA Using Mesoporous Silica Nanoparticles to Differentiate Induced Pluripotent Stem Cells into Dopaminergic Neurons. *J. Mater. Chem. B* **2017**, *5*, 3012–3023.

(20) Xia, T.; Kovochich, M.; Liong, M.; Meng, H.; Kabehie, S.; George, S.; Zink, J. I.; Nel, A. E. Polyethyleneimine Coating Enhances the Cellular Uptake of Mesoporous Silica Nanoparticles and Allows Safe Delivery of siRNA and DNA Constructs. *ACS Nano* **2009**, *3*, 3273–3286.

(21) Wu, M.; Meng, Q.; Chen, Y.; Du, Y.; Zhang, L.; Li, Y.; Zhang, L.; Shi, J. Large-Pore Ultrasmall Mesoporous Organosilica Nanoparticles: Micelle/precursor Co-Templating Assembly and Nuclear-Targeted Gene Delivery. *Adv. Mater.* **2015**, *27*, 215–222.

(22) Chen, Y. P.; Chen, C. T.; Hung, Y.; Chou, C. M.; Liu, T. P.; Liang, M. R.; Chen, C. T.; Mou, C. Y. A New Strategy for Intracellular Delivery of Enzyme Using Mesoporous Silica Nanoparticles: Superoxide Dismutase. *J. Am. Chem. Soc.* **2013**, *135*, 1516–1523.

(23) Tu, J.; Boyle, A. L.; Friedrich, H.; Bomans, P. H. H.; Bussmann, J.; Sommerdijk, N. A. J. M.; Jiskoot, W.; Kros, A. Mesoporous Silica Nanoparticles with Large Pores for the Encapsulation and Release of Proteins. *ACS Appl. Mater. Interfaces* **2016**, *8*, 32211–32219.

(24) Chen, F.; Hong, H.; Zhang, Y.; Valdovinos, H. F.; Shi, S.; Kwon, G. S.; Theuer, C. P.; Barnhart, T. E.; Cai, W. In Vivo Tumor Targeting and Image-Guided Drug Delivery with Antibody-Conjugated, Radiolabeled Mesoporous Silica Nanoparticles. *ACS Nano* **2013**, *7*, 9027–9039.

(25) Qu, Q.; Ma, X.; Zhao, Y. Anticancer Effect of α-Tocopheryl Succinate Delivered by Mitochondria-Targeted Mesoporous Silica Nanoparticles. *ACS Appl. Mater. Interfaces* **2016**, *8*, 34261–34269.

(26) Liong, M.; Lu, J.; Kovochich, M.; Xia, T.; Ruehm, S. G.; Nel, A. E.; Tamanoi, F.; Zink, J. I. Multifunctional Inorganic Nanoparticles for Imaging, Targeting, and Drug Delivery. *ACS Nano* **2008**, *2*, 889–896.

(27) Guardado-Alvarez, T. M.; Chen, W.; Norton, A. E.; Russell, M. M.; Connick, W. B.; Zink, J. I. Analyte-Responsive Gated Hollow Mesoporous Silica Nanoparticles Exhibiting Inverse Functionality and an AND Logic Response. *Nanoscale* **2016**, *8*, 18296–18300.

(28) Kwon, D.; Cha, B. G.; Cho, Y.; Min, J.; Park, E. B.; Kang, S. J.; Kim, J. Extra-Large Pore Mesoporous Silica Nanoparticles for Directing in Vivo M2 Macrophage Polarization by Delivering IL-4. *Nano Lett.* **2017**, *17*, 2747–2756.

(29) Kamkaew, A.; Cheng, L.; Goel, S.; Valdovinos, H. F.; Barnhart, T. E.; Liu, Z.; Cai, W. Cerenkov Radiation Induced Photodynamic Therapy Using Chlorin e6-Loaded Hollow Mesoporous Silica Nanoparticles. *ACS Appl. Mater. Interfaces* **2016**, *8*, 26630–26637.

(30) Kempen, P. J.; Greasley, S.; Parker, K. A.; Campbell, J. L.; Chang, H. Y.; Jones, J. R.; Sinclair, R.; Gambhir, S. S.; Jokerst, J. V. Theranostic Mesoporous Silica Nanoparticles Biodegrade after pro-Survival Drug Delivery and Ultrasound/magnetic Resonance Imaging of Stem Cells. *Theranostics* **2015**, *5*, 631–642.

(31) Rühle, B.; Datz, S.; Argyo, C.; Bein, T.; Zink, J. I. A Molecular Nanocap Activated by Superparamagnetic Heating for Externally Stimulated Cargo Release. *Chem. Commun.* **2016**, *52*, 1843–1846.

(32) Hwang, A. A.; Lee, B. Y.; Clemens, D. L.; Dillon, B. J.; Zink, J. I.; Horwitz, M. A. Tuberculosis: pH-Responsive Isoniazid-Loaded Nanoparticles Markedly Improve Tuberculosis Treatment in Mice. *Small* **2015**, *11*, 5066–5078.

(33) Paris, J. L.; Cabanas, M. V.; Manzano, M.; Vallet-Regí, M. Polymer-Grafted Mesoporous Silica Nanoparticles as Ultrasound-Responsive Drug Carriers. *ACS Nano* **2015**, *9*, 11023–11033.

(34) Li, H.; Tan, L.-L.; Jia, P.; Li, Q.-L.; Sun, Y.-L.; Zhang, J.; Ning, Y.-Q.; Yu, J.; Yang, Y.-W. Near-Infrared Light-Responsive Supramolecular Nanovalve Based on Mesoporous Silica-Coated Gold Nanorods. *Chem. Sci.* **2014**, *5*, 2804–2808.

(35) Thomas, C. R.; Ferris, D. P.; Lee, J. H.; Choi, E.; Cho, M. H.; Kim, E. S.; Stoddart, J. F.; Shin, J. S.; Cheon, J.; Zink, J. I. Noninvasive Remote-Controlled Release of Drug Molecules in Vitro Using Magnetic Actuation of Mechanized Nanoparticles. *J. Am. Chem. Soc.* **2010**, *132*, 10623–10625.

(36) Wang, H.; Wang, K.; Tian, B.; Revia, R.; Mu, Q.; Jeon, M.; Chang, F. C.; Zhang, M. Preloading of Hydrophobic Anticancer Drug into Multifunctional Nanocarrier for Multimodal Imaging, NIR-Responsive Drug Release, and Synergistic Therapy. *Small* **2016**, *12*, 6388–6397.

(37) Palanikumar, L.; Kim, H. Y.; Oh, J. Y.; Thomas, A. P.; Choi, E. S.; Jeena, M. T.; Joo, S. H.; Ryu, J. H. Noncovalent Surface Locking of Mesoporous Silica Nanoparticles for Exceptionally High Hydrophobic Drug Loading and Enhanced Colloidal Stability. *Biomacromolecules* **2015**, *16*, 2701–2714.

(38) Jiao, Y.; Sun, Y.; Tang, X.; Ren, Q.; Yang, W. Tumor-Targeting Multifunctional Rattle-Type Theranostic Nanoparticles for MRI/NIRF Bimodal Imaging and Delivery of Hydrophobic Drugs. *Small* **2015**, *11*, 1962–1974.

(39) Neuberg, C. Hydrotropic Phenomena. I. *Biochem. Z.* **1916**, *76*, 107–176.

(40) Kim, J. Y.; Kim, S.; Papp, M.; Park, K.; Pinal, R. Hydrotropic Solubilization of Poorly Water-Soluble Drugs. *J. Pharm. Sci.* **2010**, *99*, 3953–3965.

(41) Shimizu, S.; Matubayasi, N. The Origin of Cooperative Solubilisation by Hydrotropes. *Phys. Chem. Chem. Phys.* **2016**, *18*, 25621–25628.

(42) Subbarao, C. V.; Chakravarthy, I. P. K.; Sai Bharadwaj, A. V. S. L.; Prasad, K. M. M. Functions of Hydrotropes in Solutions. *Chem. Eng. Technol.* **2012**, *35*, 225–237.

(43) Das, S.; Paul, S. Mechanism of Hydrotropic Action of Hydrotrope Sodium Cumene Sulfonate on the Solubility of Di-T-Butyl-Methane: A Molecular Dynamics Simulation Study. *J. Phys. Chem. B* **2016**, *120*, 173–183.

(44) Booth, J. J.; Omar, M.; Abbott, S.; Shimizu, S. Hydrotrope Accumulation around the Drug: the Driving Force for Solubilization and Minimum Hydrotrope Concentration for Nicotinamide and Urea. *Phys. Chem. Chem. Phys.* **2015**, *17*, 8028–8037.

(45) Das, S.; Paul, S. Exploring Molecular Insights into Aggregation of Hydrotrope Sodium Cumene Sulfonate in Aqueous Solution: A Molecular Dynamics Simulation Study. *J. Phys. Chem. B*, **2015**, *119*, 3142–3154.

(46) Shimizu, S.; Booth, J. J.; Abbott, S. Hydrotrope: Binding Models vs. Statistical Thermodynamics. *Phys. Chem. Chem. Phys.* **2013**, *15*, 20625–20632.

(47) Shimizu, S.; Matubayasi, N. Hydrotropy: Monomer-Micelle Equilibrium and Minimum Hydrotrope Concentration. *J. Phys. Chem. B*, **2014**, *118*, 10515–10524

(48) Patel, A.; Malinovska, L.; Saha, S.; Wang, J.; Alberti, S.; Krishnan, Y.; Hyman, A. A. Biochemistry: ATP as a Biological Hydrotrope. *Science* **2017**, *356*, 753–756.

(49) Dalcolmo, M.; Gayoso, R.; Sotgiu, G.; D'Ambrosio, L.; Rocha, J. L.; Borga, L.; Fandinho, F.; Braga, J. U.; Galesi, V. M. N.; Barreira, D.; Sanchez, D. A.; Dockhorn, F.; Centis, R.; Caminero, J. A.; Migliori, G. B. Effectiveness and Safety of Clofazimine in Multidrug-Resistant Tuberculosis: A Nationwide Report from Brazil. *Eur. Respir. J.* **2017**, *49*, 1602445.

(50) Lechartier, B.; Cole, S. T. Mode of Action of Clofazimine and Combination Therapy with Benzothiazinones against Mycobacterium Tuberculosis. *Antimicrob. Agents Chemother.* **2015**, *59*, 4457–4463.

(51) Tyagi, S.; Ammerman, N. C.; Li, S.-Y.; Adamson, J.; Converse, P. J.; Swanson, R. V.; Almeida, D. V.; Grosset, J. H. Clofazimine Shortens the Duration of the First-Line Treatment Regimen for Experimental Chemotherapy of Tuberculosis. *Proc. Natl. Acad. Sci. USA* **2015**, *112*, 869–874.

(52) Cholo, M. C.; Steel, H. C.; Fourie, P. B.; Germishuizen, W. A.; Anderson, R. Clofazimine: Current Status and Future Prospects. *J. Antimicrob. Chemother.* **2012**, *67*, 290–298.

(53) WHO. *WHO Global Tuberculosis Report 2016*; 2016.

(54) Clemens, D. L.; Lee, B. Y.; Xue, M.; Thomas, C. R.; Meng, H.; Ferris, D.; Nel, A. E.; Zink, J. I.; Horwitz, M. A. Targeted Intracellular Delivery of Antituberculosis Drugs to Mycobacterium Tuberculosis-Infected Macrophages via Functionalized Mesoporous Silica Nanoparticles. *Antimicrob. Agents Chemother.* **2012**, *56*, 2535–2545.

(55) Huang, W. Y.; Zink, J. I. Effect of Pore Wall Charge and Probe Molecule Size on Molecular Motion inside Mesoporous Silica Nanoparticles. *J. Phys. Chem. C* **2016**, *120*, 23780–23787.

(56) Koo, H.; Min, K. H.; Lee, S. C.; Park, J. H.; Park, K.; Jeong, S. Y.; Choi, K.; Kwon, I. C.; Kim, K. Enhanced Drug-Loading and Therapeutic Efficacy of Hydrotropic Oligomer-Conjugated Glycol Chitosan Nanoparticles for Tumor-Targeted Paclitaxel Delivery. *J. Control. Release* **2013**, *172*, 823–831.

(57) Gao, L.; Gao, L.; Fan, M.; Li, Q.; Jin, J.; Wang, J.; Lu, W.; Yu, L.; Yan, Z.; Wang, Y. Hydrotropic Polymer-Based Paclitaxel-Loaded Self-Assembled Nanoparticles: Preparation and Biological Evaluation. *RSC Adv.* **2017**, *7*, 33248–33256.

(58) Lee, S. C.; Huh, K. M.; Lee, J.; Cho, Y. W.; Galinsky, R. E.; Park, K. Hydrotropic Polymeric Micelles for Enhanced Paclitaxel Solubility: In Vitro and in Vivo Characterization. *Biomacromolecules* **2007**, *8*, 202–208.

(59) Huh, K. M.; Lee, S. C.; Cho, Y. W.; Lee, J.; Jeong, J. H.; Park, K. Hydrotropic Polymer Micelle System for Delivery of Paclitaxel. *J. Control. Release* **2005**, *101*, 59–68.

(60) Lee, J.; Lee, S. C.; Acharya, G.; Chang, C. J.; Park, K. Hydrotropic Solubilization of Paclitaxel: Analysis of Chemical Structures for Hydrotropic Property. *Pharm. Res.* **2003**, *20*, 1022–1030.

Table of Contents